



Fabrication and mechanical properties of $Ti_2AlC/TiAl$ composites with co-continuous network structure

Li-rong REN^{1,2}, Shui-jie QIN¹, Si-hao ZHAO¹, Hua-qiang XIAO¹

1. School of Mechanical Engineering, Guizhou University, Guiyang 550025, China;

2. School of Mechatronics Engineering, Guizhou Minzu University, Guiyang 550025, China

Received 7 August 2020; accepted 28 January 2021

Abstract: $Ti_2AlC/TiAl$ composites with different volume fractions were prepared by hot pressing technology, and their reinforced structural characteristics and mechanical properties were evaluated. The results showed that when the reinforced phase volume fraction of Ti_2AlC was 20%, three-dimensional interpenetrating network structures were formed in the composites. Above 20%, Ti_2AlC phase in the composites accumulated and grew to form thick skeletal networks. The microplastic deformation behavior of Ti_2AlC phase, such as kink band and delamination, improved the fracture toughness of the composites. Comparative analysis indicated that the uniform and small interconnecting network structures could further reinforce the composites. The bending strengths of composites prepared with 20 vol.% Ti_2AlC reached (900.9±45.0) MPa, which was 25.5% higher than that of $TiAl$ matrix. In general, the co-continuous $Ti_2AlC/TiAl$ composite with excellent mechanical properties can be prepared by powder metallurgy method.

Key words: $Ti_2AlC/TiAl$ composites; co-continuous composites; hot pressing; strengthening mechanism

1 Introduction

$TiAl$ alloys possess remarkable properties including low density, high creep, and superior strength at elevated temperatures. Therefore, $TiAl$ alloys are expected to partially replace nickel-based superalloys at temperatures of 600–950 °C. So far, $TiAl$ alloys have been successfully used in aero-engine blades, supercharged impeller, and exhaust valves [1]. However, their low plasticity at room temperature restricts their large-scale applications. Notably, the mechanical properties of alloys can often be improved by adding metallic elements (such as Nb, Mo, Ta, and W) [2–4] or non-metallic elements (such as B, C, and Si) [5,6]. In recent years, $TiAl$ intermetallic matrix composites (IMCs) have attracted increasing attention due to their tailored microstructures and enhanced mechanical

properties [7–9]. Integrating the advantages of both ceramic and metal, MAX phase (M is a transition metal, A is an A-group element, and X is nitrogen or carbon) exhibits not only good high-temperature stability, but also capability to improve the toughness of $TiAl$ composites at room temperature, through micro-plastic deformation mechanism. CHEN et al [10] and YANG et al [11] synthesized $Ti_2AlC/TiAl$ composites via in situ hot pressing and studied the in situ synthesis mechanism of composites, respectively. LAPIN et al [12,13] used centrifugal casting to prepare in situ $Ti_2AlC/TiAl$ composites. Their results suggested improvement in creep properties of composites due to the formation of the granular Ti_2AlC phase. SONG et al [14] employed vacuum arc melting to obtain $Ti_2AlC/TiAl$ composites with improved strength and plasticity under the cooperative contribution of TiC and Ti_2AlC .

Compared to other composite structures, IMCs with interpenetrating structures have better strength, toughness, and wear resistance. CHENG et al [15] and WANG et al [16] prepared $\text{Ti}_2\text{AlC}/\text{TiAl}$ and $\text{Ti}_2\text{AlN}/\text{TiAl}$ composites with three-dimensional network structures by in situ synthesis technology to yield composites with excellent wear resistance. On the other hand, co-continuous IMCs with a high melting point are usually prepared by in situ synthesis technologies. The microstructures and properties of obtained composite materials are significantly influenced by the exothermic reaction, residual reactants, and/or intermediates.

In this study, commercial Ti4822 alloy powder and Ti_2AlC powder were used as raw materials to prepare three-dimensional interpenetrating network structure composites. The formation of Ti_2AlC network reinforcement structure and its effects on the mechanical properties of the as-obtained composites were evaluated at room temperature. The study is expected to provide guidance for the preparation of co-continuous IMCs with high melting point by powder metallurgy method.

2 Experimental

2.1 Materials

Ti4822 (0–20 μm , atomized powder, Ti 60.34 wt.%, Al 32.30 wt.%, Nb 4.51 wt.%, Cr 2.85 wt.%) and Ti_2AlC (<75 μm , vacuum sintering) powders were employed as raw materials. Figure 1 shows scanning electron microscopy (SEM) images of the powders, revealing that the sphericity of the particles of TiAl powder was relatively high; however, the surface of Ti_2AlC prepared by vacuum sintering exhibited typical quasi-plastic deformation characteristics such as layered delamination and kink band. Different composite powders were prepared by varying the volume fractions of the two powders. The specific composition of each sample is listed in Table 1.

The procedure consisted of putting the powders in stainless steel ball milling tank filled with argon for ball grinding. The ball/material mass ratio was set at 5:1, rotation speed at 300 r/min, and ball milling time at 2 h. After sieving and drying, the resulting powder was placed in a graphite mold (30 mm in diameter) and sintered in vacuum hot pressing furnace. During sintering, the furnace temperature was firstly increased to 600 °C at a

heating rate of 10 °C/min followed by 1000 °C at 20 °C/min, 1150 °C at 10 °C/min and maintained for 1 h, then to 800 °C at 10 °C/min, and finally to room temperature during furnace cooling. The furnace pressure during this process was set at 30 MPa. After completion of insulation, the pressure was removed to yield samples with a diameter of 30 mm and a height of 10 mm.

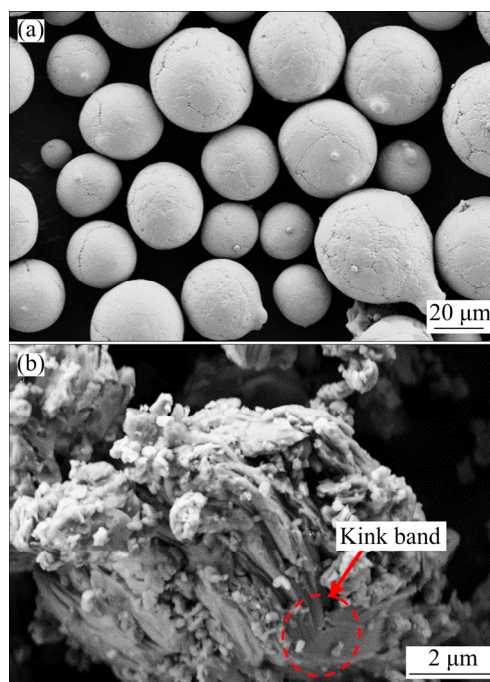


Fig. 1 SEM images of powders: (a) Ti4822; (b) Ti_2AlC

Table 1 Chemical compositions of composites (vol.%)

Sample ID	TiAl	Ti_2AlC
TAC0	100	0
TAC10	90	10
TAC20	80	20
TAC30	70	30
TAC40	60	40

2.2 Characterization

The specimens used for mechanical properties measurements were prepared by electrical discharge machining. Room temperature compression and three-point bending tests were carried out using an INSTRON 5569 testing system. The dimensions of specimens used for compression tests were $d4 \text{ mm} \times 6 \text{ mm}$ at a constant strain rate of 10^{-3} s^{-1} . The dimensions of specimens employed for flexural strength testing were $2 \text{ mm} \times 4 \text{ mm} \times 20 \text{ mm}$. The bars were loaded with spans of 10 mm, and

crosshead speed utilized for bending strength testing was 0.5 mm/min.

The microstructural characterization was performed by field-emission SEM (Quanta FEG 250). $V(\text{HF}):V(\text{HNO}_3):V(\text{H}_2\text{O})$ at the ratio of 1:3:6 was used as metallographic etchant, and pure HF was employed for deep etching. The phase compositions were analyzed by X-ray diffraction (XRD, D8-Advance, Bruker). The specimens with dimensions of 10 mm × 10 mm × 5 mm were cut by electrical discharge machining and polished to 1 μm. The hardness measurements were collected on a Vickers hardness machine (430SVA, Wilson Wolpert) using a 1 kg load for 10 s.

3 Results and discussion

3.1 Phase composition

XRD patterns of the TiAl alloys and $\text{Ti}_2\text{AlC}/\text{TiAl}$ composites prepared with different Ti_2AlC contents after sintering are presented in Fig. 2. The matrix of the alloy contained $\alpha_2\text{-Ti}_3\text{Al}$ and $\gamma\text{-TiAl}$ phases, and volume fraction of Ti_2AlC phase was significantly increased in the composites. With the increase in the volume fraction of Ti_2AlC , the intensity of Ti_2AlC peak was significantly enhanced for composites. Unlike $\text{Ti}_2\text{AlC}/\text{TiAl}$ composites prepared by in situ reaction, composites obtained herein contained only $\gamma\text{-TiAl}$, $\alpha_2\text{-Ti}_3\text{Al}$, and Ti_2AlC phases. No other intermediate products, such as TiAl_3 , Ti_2Al_5 , Ti_3AlC , and Ti_3AlC_2 were noticed. Moreover, no unreacted Ti, C and TiC phase were recorded, indicating the formation of composites with fewer impurities.

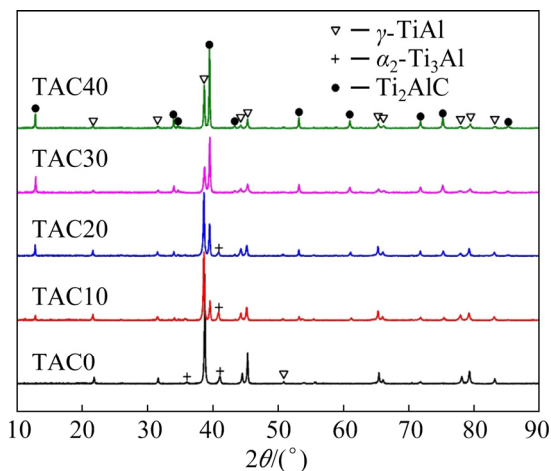


Fig. 2 XRD patterns of TiAl alloy and $\text{Ti}_2\text{AlC}/\text{TiAl}$ composites

3.2 Microstructures

Microstructural images of the substrate and composite materials prepared with different Ti_2AlC contents are provided in Fig. 3. The Ti4822 substrate was composed entirely of $\alpha_2+\gamma$ lamellar structure and the diameters of $\alpha_2+\gamma$ lamellar colonies exceeded 300 μm (Fig. 3(a)). Composite materials appeared to be compact without holes. The morphological characteristics showed different forms of Ti_2AlC phase distributed in $\alpha_2+\gamma$ lamellar colonies. At low Ti_2AlC contents, Ti_2AlC phase was distributed as small dispersed particles at the boundaries of $\alpha_2+\gamma$ lamellar colonies with diameters of around 3 μm (Fig. 3(b)). At Ti_2AlC phase content of 20 vol.%, most Ti_2AlC particles became interlinked to form obvious network structures with the exception of some isolated Ti_2AlC particles with sizes ranging from 3 to 6 μm. At Ti_2AlC content of 30 vol.%, Ti_2AlC particles with sizes around 6 μm completely formed three-dimensional network morphologies. Moreover, some Ti_2AlC particles aggregated and grew to yield blocky structures with diameters above 10 μm. With further increase in the Ti_2AlC phase content to 40 vol.%, Ti_2AlC phase in the composite material completely aggregated and grew to form larger network structures. Figure 3(f) shows the partial enlarged drawing of Ti_2AlC network in TAC40, revealing the existence of a small number of particles at the interface between Ti_2AlC skeleton and the substrate, which might be the Al_2O_3 impurity introduced during the material preparation process.

To further investigate the three-dimensional reinforced composite structures, the characteristics of Ti_2AlC -reinforced phase after removal of TiAl matrix by deep etching were evaluated and the results are presented in Fig. 4. At Ti_2AlC phase content of 10 vol.%, dispersed particles were mainly noticed. At Ti_2AlC phase contents exceeding 20 vol.%, the reinforced phase Ti_2AlC formed obvious three-dimensional interpenetration network structures (Figs. 4(b–d)). With further increase in the content, the Ti_2AlC phase gradually accumulated and grew to form thick skeletal network structures. Therefore, the three-dimensional continuous interpenetrating network structures of Ti_2AlC reinforcement and TiAl matrix were obtained by hot pressing. On the other hand, the characteristics of the interpenetrating network

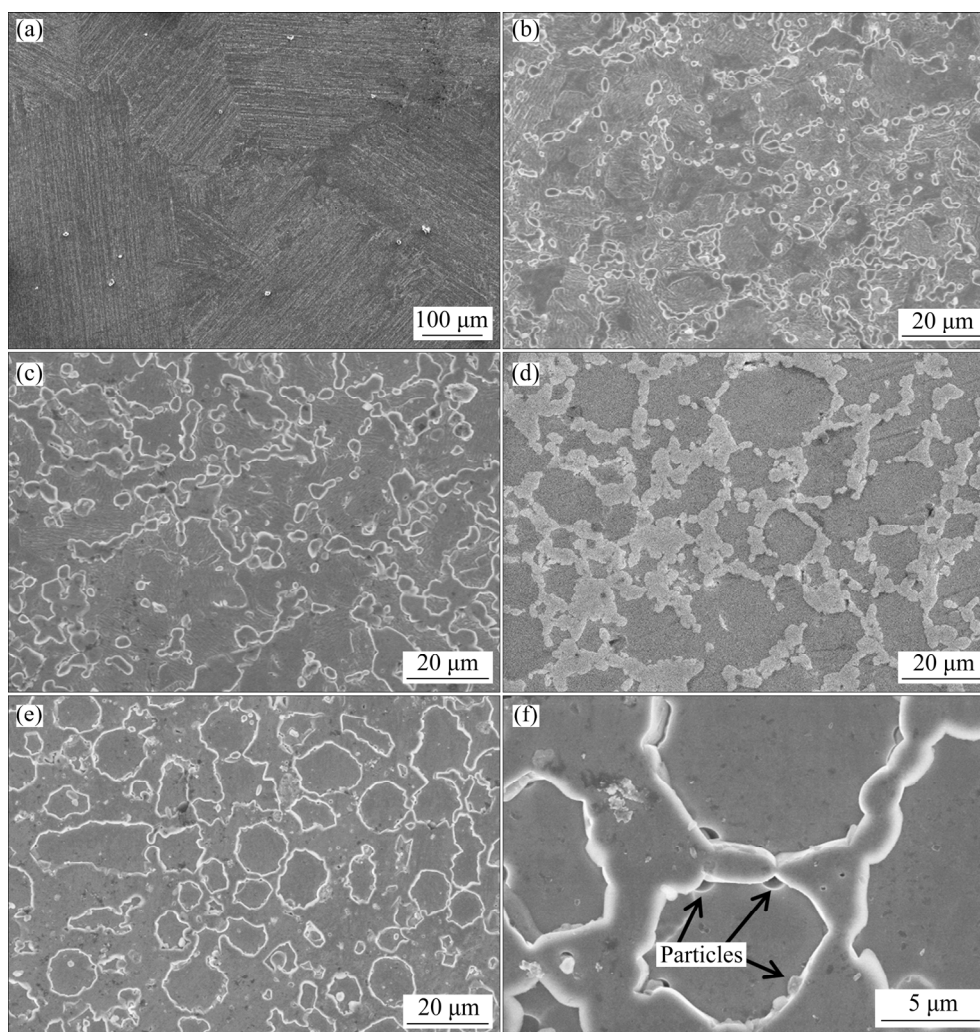


Fig. 3 SEM micrographs of TiAl and $\text{Ti}_2\text{AlC}/\text{TiAl}$ composites: (a) TAC0; (b) TAC10; (c) TAC20; (d) TAC30; (e) TAC40; (f) High magnification image of Ti_2AlC network and Al_2O_3 particles

structure and scale of reinforcing phase could be adjusted by the content of reinforcing phase. Consequently, the regulation of the microstructures and properties of high melting point co-continuous composites was achieved by powder metallurgy technology.

3.3 Mechanical properties

The Vickers hardness values of the alloy and composites are illustrated in Fig. 5. Significant increase in hardness was observed after the addition of Ti_2AlC reinforcement. Compared to TiAl matrix, the Vickers hardness values of TAC10 and TAC20 were enhanced by about 30%, and those of TAC30 and TAC40 by 38% and 55% (similar to HV 567.5), respectively. Thus, harder Ti_2AlC reinforcement significantly increased the deformation resistance inside the composite material. Besides, two

interconnected structures formed by high volume fraction Ti_2AlC reinforcement led to the production of interlock structures, further improving the deformation resistance of the composites. The introduction of Ti_2AlC also resulted in the effective increase on the phase refinement scale of $\alpha_2+\gamma$ lamellar colonies, thereby enhancing the carrying capacity of substrates.

Typical compressive stress–strain and flexural strength–deflection curves of TiAl alloy and $\text{Ti}_2\text{AlC}/\text{TiAl}$ composites at room temperature are shown in Fig. 6. The matrix displayed good compressive strength and compression plasticity (Fig. 6(a)). The compressive strength of the matrix was close to 1800 MPa but both compressive yield strength and elastic modulus were relatively low. The introduction of Ti_2AlC phase significantly improved the yield strength and elastic modulus of

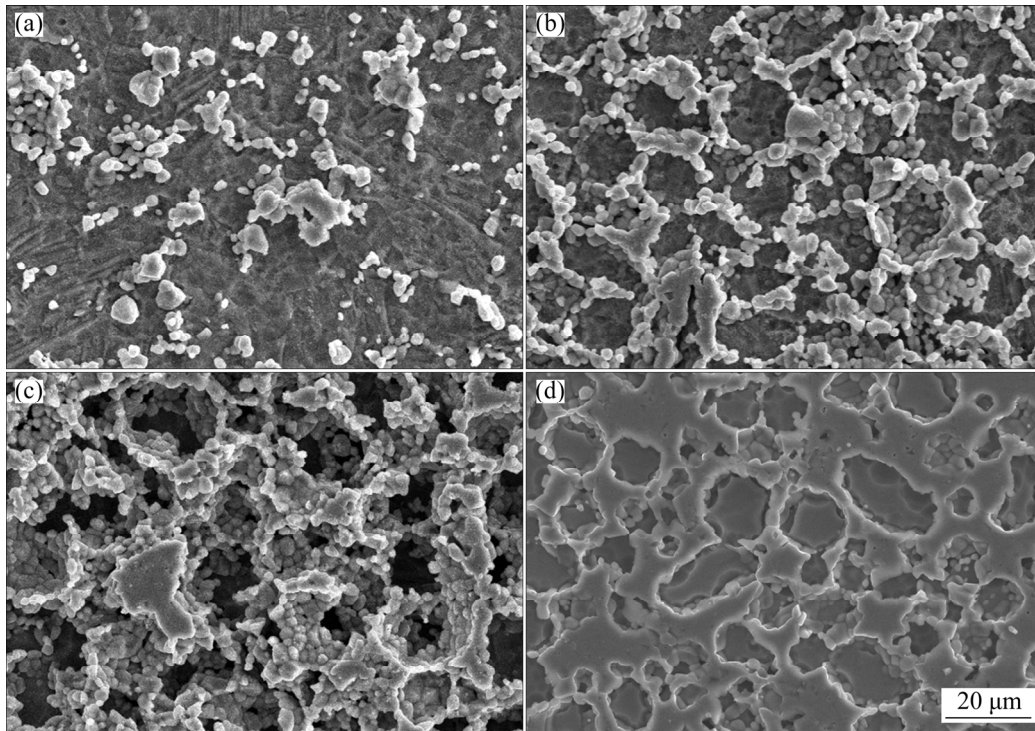


Fig. 4 SEM images of Ti_2AlC after etching of TiAl substrate: (a) TAC10; (b) TAC20; (c) TAC30; (d) TAC40

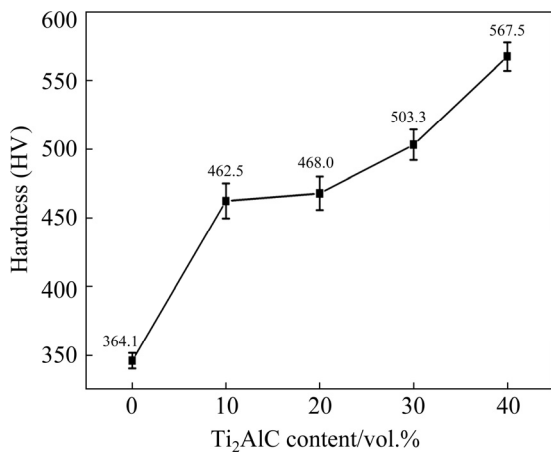


Fig. 5 Vickers hardness of TiAl alloy and $\text{Ti}_2\text{AlC}/\text{TiAl}$ composites

the material. Figure 6(a) exhibits the compression curves, demonstrating that the offset yield strengths of composites TAC10, TAC20, TAC30 and TAC40 were 1090, 1105, 1145, and 1195 MPa, respectively. Moreover, the compressive yield strengths of the composites were all above 1000 MPa. This value was two times that of TiAl matrix and increased gradually with the increase in the content of reinforcement phase. At low Ti_2AlC phase contents (TAC10 and TAC20), the composites illustrated better compression plasticity and higher compressive strength. At higher Ti_2AlC phase

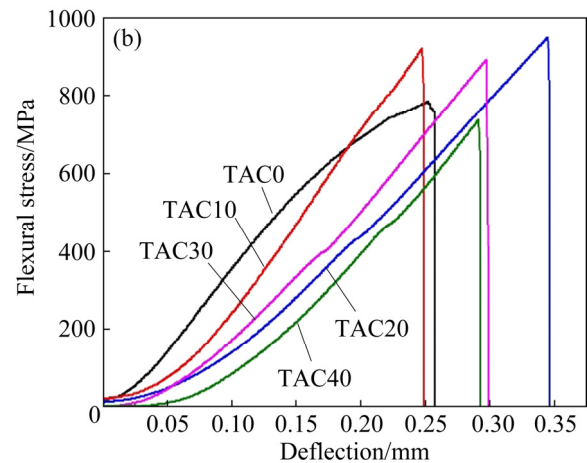
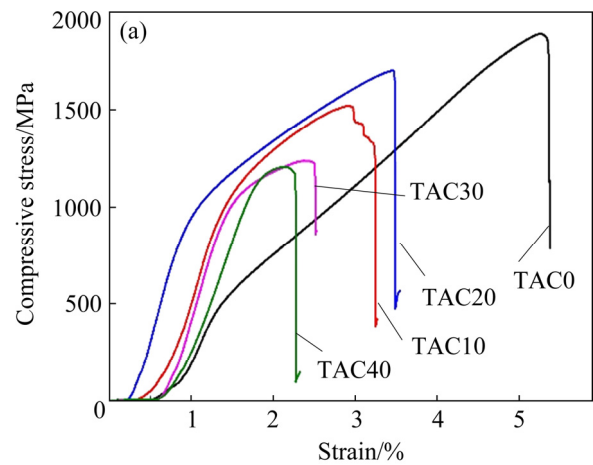


Fig. 6 Compressive (a) and bending (b) curves of TiAl alloy and $\text{Ti}_2\text{AlC}/\text{TiAl}$ composites at room temperature

contents (TAC30 and TAC40), the compression plasticity and compressive strength of the composites decreased obviously, and TAC20 showed the best values among several prepared composite materials.

The results of three-point bending resistance tests are presented in Fig. 6(b). TiAl alloy and Ti₂AlC/TiAl composites showed obvious brittle fracture characteristics. The bending strengths of other composites were significantly higher than that of TiAl alloy matrix except that of TAC40 composite.

To evaluate the effects of Ti₂AlC phase content on the mechanical properties of composites, the compressive and flexural strengths of TiAl alloy and Ti₂AlC/TiAl composites were obtained at room temperature. Figure 7 demonstrates that the matrix displays the highest compressive strength ((1797.5±65.9) MPa). After the addition of Ti₂AlC at 10 or 20 vol.%, the compressive strength of the composites gradually declined to about 1500 MPa. With the increase in the content of Ti₂AlC to 30 or 40 vol.%, the compressive strength of the composites decreased significantly to about 1200 MPa. Unlike the variation law of compressive strength, Ti₂AlC significantly improved the three-point bending strengths of the composites except TAC40. Compared to that of TiAl matrix, the bending strengths of TAC10, TAC20, and TAC30 were found to increase by 16.7%, 25.5%, and 20.5%, respectively. The bending strength of TAC20 was the highest ((900.9±45.0) MPa), which was much higher than that of the composites fabricated by reactive hot pressing [15]. Therefore, TAC20 composite showed the highest flexural

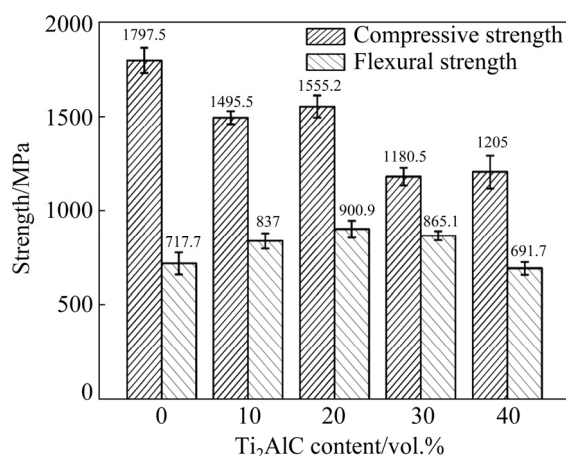


Fig. 7 Compressive and flexural strengths of TiAl alloy and Ti₂AlC/TiAl composites

strength while maintaining elevated compressive strength, indicating better comprehensive mechanical properties.

3.4 Fractograph and strengthening mechanism

Typical translamellar and interlamellar fractures in TiAl alloy are provided in Fig. 8(a). The microfracture morphologies showed interlaced serrated sections, while the macrofracture morphologies displayed uneven steps between different $\alpha_2+\gamma$ lamellar colonies. The mechanical properties of TiAl alloys were mainly determined by the size of lamellar colonies, as well as lamellar spacing of $\alpha_2+\gamma$ lamellar structure. Figures 8(b–e) exhibit that the macroscopic sections of the composites are flat with obvious brittle fracture characteristics. Steps caused by partial crack deflection were observed on sections of TAC10, TAC20 and TAC30, while TAC40 appeared with completely flat and brittle fracture. Therefore, the microscopic fracture characteristics showed fractures consisting of large cleavage plane, bright white tearing edge, and local river pattern. The dark gray cleavage plane and local river pattern were associated with the fracture characteristics of TiAl matrix; however, the bright white tearing edge reflected the micro plastic fracture behavior of Ti₂AlC phase.

The existence of numerous cleavage steps and tensile tearing regions on the fracture surface indicated that the introduction of Ti₂AlC phase could enhance the quasi-cleavage fracture of TiAl matrix. Moreover, the introduced Ti₂AlC phase was characterized by typical microscopic plastic deformation mechanisms, such as kink band and delamination, as well as particle pull-out and crack deflection behavior (Fig. 8(f)). The transformation of such fracture behaviors provided the composites with high fracture and damage tolerance, thereby better strengthening.

The enhanced structural characteristics of Ti₂AlC phase also impacted the fracture behavior of the composites. Isolated Ti₂AlC phase in TAC10 coordinated the deformation of lamellar colonies and played an enhancing role. The enhancement of Ti₂AlC particles was reflected in the refinement of the TiAl substrate on the one hand and the enhancement of the load transfer on the other hand. The network-like Ti₂AlC structures of TAC20 and TAC30 composites not only provided sufficient

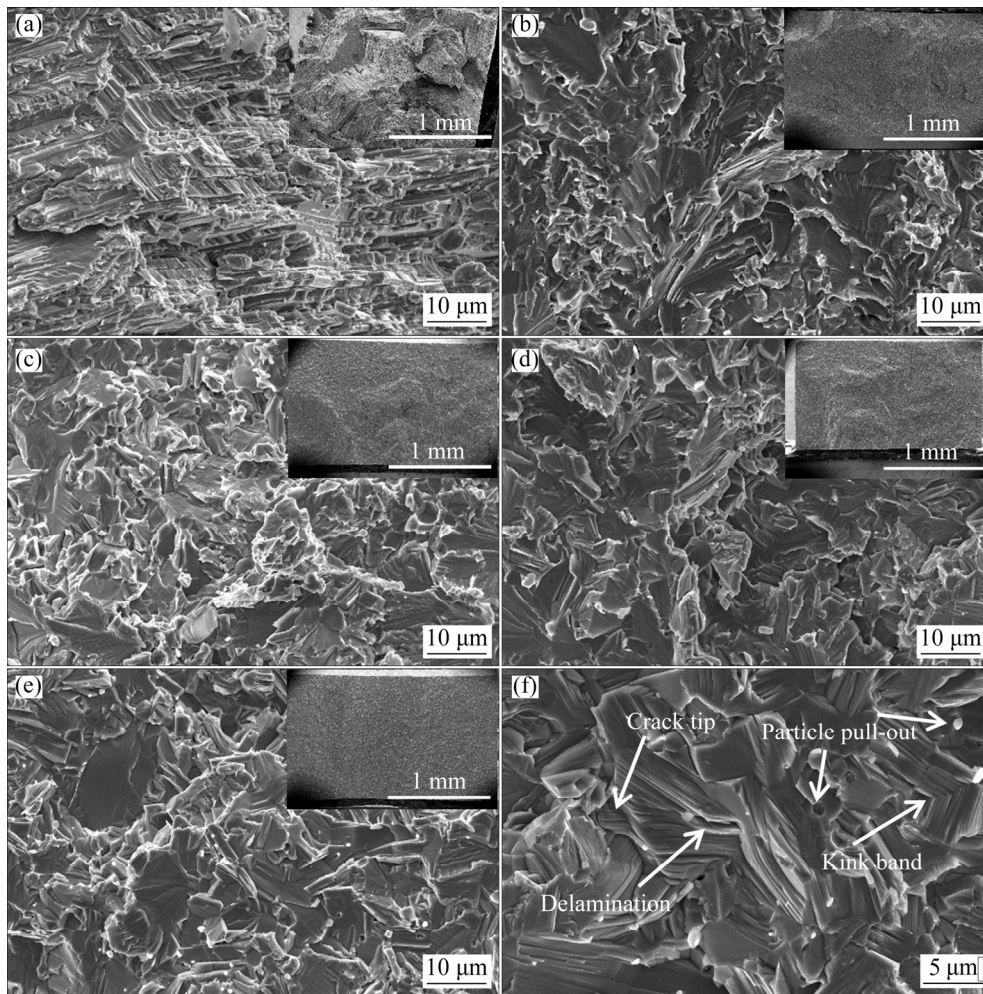


Fig. 8 Fracture morphologies of TiAl alloy and $\text{Ti}_2\text{AlC}/\text{TiAl}$ composites: (a) TAC0; (b) TAC10; (c) TAC20; (d) TAC30; (e) TAC40; (f) High magnification of Ti_2AlC fracture surface

microscopic toughening mechanism but also realized certain interlock function of the two-phase three-dimensional interpenetrating structure. This, in turn, yielded better strengthening role and improved comprehensive mechanical properties. For TAC40, the thick Ti_2AlC network skeleton structure weakened the bearing capacity of the matrix, and prior crack propagation in the skeleton yielded composites with poor compressive and bending abilities. Therefore, uniform and fine two-phase interpenetrating structures were obtained by adjusting the volume fraction of the reinforcing phase. This further improved the comprehensive mechanical properties of $\text{Ti}_2\text{AlC}/\text{TiAl}$ composites.

4 Conclusions

(1) The increase in volume fraction of the reinforcing phase resulted in the change in the

reinforced structure of the $\text{Ti}_2\text{AlC}/\text{TiAl}$ composite from particle reinforcement to two-phase co-continuous network structure.

(2) The microplastic deformation mechanism of Ti_2AlC phase and its transformation to coordinate the deformation behavior of TiAl matrix yielded composites with high fracture and damage tolerance, thereby better strengthening effect.

(3) Appropriate reinforcing phase volume fraction was a key parameter to obtain uniform and fine interpenetrating structures, which is expected to further improve the comprehensive mechanical properties of $\text{Ti}_2\text{AlC}/\text{TiAl}$ composites.

Acknowledgments

The authors are grateful for the financial supports from the National Natural Science Foundation of China (No. 52065009), the Joint Funds of the Science and Technology Foundation of

Guizhou Province, China (No. 20157219), and the Science and Technology Planning Project of Guizhou Province, China (No. 20191069).

References

- [1] YANG Rui. Advances and challenges of TiAl base alloys [J]. Acta Metallurgica Sinica, 2015, 51(2): 129–147. (in Chinese)
- [2] ISMAEEL A, WANG C S. Effect of Nb additions on microstructure and properties of γ -TiAl based alloys fabricated by selective laser melting [J]. Transactions Nonferrous Metals Society of China, 2019, 29: 1007–1016.
- [3] NIU H Z, CHEN X J, CHEN Y F, ZHAO S, LIU G H, ZHANG D L. Microstructural stability, phase transformation and mechanical properties of a fully-lamellar microstructure of a Mo-modified high-Nb γ -TiAl alloy [J]. Materials Science and Engineering A, 2020, 784: 139313.
- [4] ZHU H L, SEO D Y, MARUYAMA K, AU P. Strengthening of a fully lamellar TiAl + W alloy by dynamic precipitation of *B* phase during long-term creep [J]. Scripta Materialia, 2006, 54: 425–430.
- [5] WANG Qi, CHEN Rui-run, YAN Hou-hua, GUO Jingjie, SU Yan-qing, DING Hong-sheng, FU Heng-zhi. Effects of V and B, Y additions on the microstructure and creep behaviour of high-Nb TiAl alloys [J]. Journal of Alloys and Compounds, 2018, 7747: 640–647.
- [6] YANG L, CHAI L H, WANG Y L, GAO S B, SONG L, LIN J P. Precipitates in high-Nb TiAl alloyed with Si [J]. Scripta Materialia, 2015, 154: 8–11.
- [7] LU Xiao-fang, LI Jian-bo, CHEN Xian-hua, QIU Jing-wei, WANG Yan, LIU Bin, LIU Yong, RASHAD M, PAN Fu-sheng. Mechanical, tribological and electrochemical corrosion properties of in-situ synthesized $\text{Al}_2\text{O}_3/\text{TiAl}$ composites [J]. Intermetallics, 2020, 120: 106758.
- [8] LI Wei, YANG Yi, LI Ming, LIU Jie, CAI Dao-sheng, WEI Qing-song, YAN Chun-ze, SHI Yu-sheng. Enhanced mechanical property with refined microstructure of a novel γ -TiAl/TiB₂ metal matrix composite (MMC) processed via hot isostatic press [J]. Materials and Design, 2018, 141: 57–66.
- [9] KAN W, CHEN B, PENG H, LIANG Y, LIN J. Fabrication of nano-TiC reinforced high Nb–TiAl nanocomposites by electron beam melting [J]. Materials Letters, 2020, 259: 126856.
- [10] CHEN Yan-lin, YAN Ming, SUN Yi-ming, MEI Bing-chu, ZHU Jiao-qun. The phase transformation and microstructure of TiAl/Ti₂AlC composites caused by hot pressing [J]. Ceramics International, 2009, 35: 1807–1812.
- [11] YANG Chen-hui, WANG Fen, AI Tao-tao, ZHU Jian-feng. Microstructure and mechanical properties of in situ TiAl/Ti₂AlC composites prepared by reactive hot pressing [J]. Ceramics International, 2014, 40: 8165–8171.
- [12] LAPIN J, KAMYSHNYKOVA K. Processing, microstructure and mechanical properties of in-situ Ti₃Al+TiAl matrix composite reinforced with Ti₂AlC particles prepared by centrifugal casting [J]. Intermetallics, 2018, 98: 34–44.
- [13] LAPIN J, KLIMOVA A, GABALCOVA Z, PELACHOVA T, BAJANA O, ŠTAMBORSKA M. Microstructure and mechanical properties of cast in-situ TiAl matrix composites reinforced with (Ti,Nb)₂AlC particles [J]. Materials and Design, 2017, 133: 404–415.
- [14] SONG Xiao-jie, CUI Hong-zhi, HAN Ye, HOU Nan, WEI Na, DING Lei, SONG Qiang. Effect of carbon reactant on microstructures and mechanical properties of TiAl/Ti₂AlC composites [J]. Materials Science and Engineering A, 2017, 684: 406–412.
- [15] CHENG Jun, ZHU Sheng-yu, YU Yuan, YANG Jun, LIU Wei-ming. Microstructure, mechanical and tribological properties of TiAl-based composites reinforced with high volume fraction of nearly network Ti₂AlC particulates [J]. Journal of Materials Science and Technology, 2018, 34: 670–678.
- [16] WANG D Q, SUN D L, HAN X L, WANG Q. In situ Ti₂AlN reinforced TiAl-based composite with a novel network structure: Microstructure and flexural property at elevated temperatures [J]. Materials Science and Engineering A, 2019, 742: 231–240.

两相连续网络结构 Ti₂AlC/TiAl 复合材料的制备及力学性能

任丽蓉^{1,2}, 秦水介¹, 赵思皓¹, 肖华强¹

1. 贵州大学 机械工程学院, 贵阳 550025; 2. 贵州民族大学 机械电子工程学院, 贵阳 550025

摘要: 采用热压工艺制备不同体积分数的 Ti₂AlC/TiAl 复合材料, 并研究其增强结构特征及力学性能。当增强相体积分数达到 20% 时, 复合材料形成两相三维互贯通的结构; 当增强相体积分数高于 20%, 复合材料中 Ti₂AlC 相聚长大并形成粗大的骨骼网络。Ti₂AlC 相的微观塑性变形行为(如扭转和层裂)能改善复合材料的断裂韧性, 均匀细小的两相互贯通网络结构使复合材料得到进一步强化。20 vol.% Ti₂AlC/TiAl 的复合材料的抗弯强度达到 (900.9±45.0) MPa, 比 TiAl 基体的提高 25.5%。采用粉末冶金工艺能制备具有优异综合力学性能的两相连续网络结构的 Ti₂AlC/TiAl 复合材料。

关键词: Ti₂AlC/TiAl 复合材料; 连续增强复合材料; 热压缩; 强化机理

(Edited by Wei-ping CHEN)